

Controlling synfire chain by inhibitory synaptic input

Author TAKASHI SHINOZAKI¹ *, Author HIDEYUKI CÂTEAU¹, Author HIDETOSHI URAKUBO² and Author MASATO OKADA^{1,3}

¹*RIKEN Brain Science Institute, Wako-shi, Saitama 351-198, Japan*

²*Graduate School of Science, University of Tokyo, Bunkyo-ku, Tokyo 113-0033, Japan*

³*Graduate School of Frontier Sciences, University of Tokyo, Kashiwa-shi, Chiba 277-8561, Japan*

The propagation of highly synchronous firings across neuronal networks, called the synfire chain, has been actively studied both theoretically and experimentally. The temporal accuracy and remarkable stability of the propagation have been repeatedly examined in previous studies. However, for such a mode of signal transduction to play a major role in processing information in the brain, the propagation should also be controlled dynamically and flexibly. Here, we show that inhibitory but not excitatory input can bidirectionally modulate the propagation, i.e., enhance or suppress the synchronous firings depending on the timing of the input. Our simulations based on the Hodgkin-Huxley neuron model demonstrate this bidirectional modulation and suggest that it should be achieved with any biologically inspired modeling. Our finding may help describe a concrete scenario of how multiple synfire chains lying in a neuronal network are appropriately controlled to perform significant information processing.

KEYWORDS: synfire chain, Hodgkin-Huxley model, rebound firing, post inhibitory enhancement, numerical analysis

1. Introduction

The synfire chain,¹⁾ which is the stable propagation of highly synchronous population firings, has been proposed to be a mechanism by which signals are transmitted in the brain and has been actively studied theoretically.²⁻¹⁴⁾ The synfire chain is expected to explain accurately the timed firings of multiple neurons observed in various brain preparations,¹⁵⁻¹⁷⁾ which are otherwise difficult to explain.

Simulation⁴⁾ and analytical⁵⁾ studies have demonstrated that this mechanism of signal transmission is certainly possible at least in the simplest feedforward circuit composed of excitatory neurons with all-to-all connections between successive layers. In this circuit, synchronous population firings, which we call a pulse packet^{4,18)} throughout the paper, propagate in either a stable mode or a fading mode. The propagating mode is solely determined by the initial synchrony level.

Following these studies, it was shown that the inclusion of inhibitory neurons with Mexican-hat-type connections added another stably propagating mode in the same feedforward circuit.¹³⁾ This idea of creating multiple stably propagating modes by appropriately choosing neural connections was further put forward systematically. It was then demonstrated that an arbitrary number of different firing modes could propagate in the feedforward circuit if the neural connections were chosen by a method analogous to the model of associative memory.^{19,20)}

Instead of creating multiple propagation modes in a single feedforward circuit, the embedding of multiple feedforward circuits in a large population of neurons gives another direction for multiplying the propagation modes.²¹⁻²³⁾ In such embedding, some group of neurons in the network can be shared by two or more feedforward

circuits. A pulse packet propagating in a feedforward circuit can therefore jump to another one via a shared group of neurons.

These multiple propagation modes, however, have a limited value if a workable mechanism to switch between different propagation modes is not available. The present paper shows that whenever neurons are modeled in a biologically inspired manner, the propagating activity can be bidirectionally modulated by inhibitory input: it is either enhanced or suppressed depending on the timing of the input.

Our simulations using a feedforward circuit consisting of Hodgkin-Huxley (HH) neurons reveal that inhibitory modulatory input to a layer in the circuit can either enhance or suppress a propagating pulse packet depending on the time lag, Δt , of the modulatory input relative to the arrival of the pulse packet at the layer. The degree of enhancement or suppression changes gradually with Δt . This ability of graded bidirectional control of pulse packet propagation is unique to the inhibitory input. Excitatory input enhances a pulse packet propagation efficiently but suppresses it poorly. It is an inappropriate modulator also because it overrides and erases the timing information carried by the propagating pulse packet, while the inhibitory input does not. We show that the bidirectional nature of inhibitory modulation stems from an outward rectifying current into the neuron existing not only in the HH model but also in virtually any biologically inspired neuron model so that the switching mechanism itself should exist universally. This flexible modulatory mechanism would be useful in switching between different propagation modes in the feedforward circuit or in switching between different feedforward circuits embedded in a network.

In the second section, we describe our simulation method, and in the third section, we show our simula-

*E-mail address: tshino@brain.riken.jp

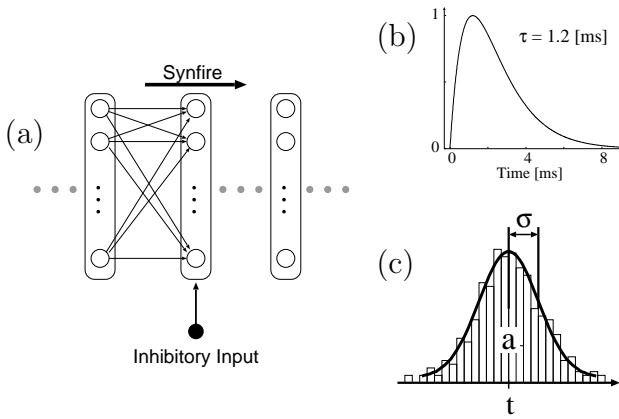


Fig. 1. (a) Feedforward circuit of excitatory neurons with modulatory input, which was used for the simulations. Layers of excitatory neurons are connected in an all-to-all manner. One or two layers of these neurons receive a uniform modulatory input, which is timed in reference to the arrival of a pulse packet at the modulated layer. (b) Schematic illustration of an alpha function with time-to-peak value $\tau = 1.2$ ms. (c) Schematic illustration of a pulse packet. The pulse packet was assembled from multiple firings that temporally formed a Gaussian distribution. The property of the pulse packet was represented by the total firing number a , time variance σ , and mean input time t .

tion results. The final section is devoted to the summary and discussion.

2. Methods

A feedforward network having a hundred excitatory neurons per layer (Fig. 1(a)) was simulated in the NEURON simulator environment.²⁴⁾ Each neuron was modeled by the HH equation²⁵⁾ (see Appendix for details). In order to mimic the noisy environment in the cortex,^{4,5)} stochastic background inputs to each neuron were also assumed: $I = I_0 + sw(t)$, where $w(t)$ is Gaussian white noise. We chose the values $I_0 = 0.45$ nA and $s^2 = 0.045$ nA² to enable the firing of neurons in a layer at a biologically plausible rate (2 Hz).

The excitatory neurons in a layer innervate to the neurons in the following layer in an all-to-all manner. The synaptic currents were modeled with an alpha function (Fig. 1(b)) $\alpha(t) = \frac{t}{\tau} \exp(-(t-\tau)/\tau) : g\alpha(t)(V-E)$, where τ is the time to the peak, g is the peak amplitude, and V is the reversal potential. We used parameter values $(\tau, g, V) = (1.2$ ms, 0.035 nS, 0 mV) for all the excitatory synapses.

Additionally, we considered modulatory inputs. They were simultaneously given to all the neurons in the modulated layer at a specified time in reference to the arrival of a pulse packet at the layer. The modulatory currents were also modeled with the alpha function with $(\tau, g, V) = (1.0$ ms, 6.0 nS, -70 mV) for the inhibitory input and $(\tau, g, V) = (1.0$ ms, 0.7 nS, 0 mV) for the excitatory input.

The histogram of the synchronous firings, pulse packet, at a layer is generally bellshaped.¹⁸⁾ In our simulations, we used a Gaussian function whose width and area are σ and a , respectively, as a pulse packet to be fed into the circuit (Fig. 1(c)). The resulting histogram of the firings

was fitted again with a Gaussian function parametrized by σ' and a' .

3. Results

Figure 2 shows how the pulse packet propagation is modulated by the inhibitory input. It is known that the synchrony level of the initial pulse packet specified by (σ, a) determines the fate of the pulse packet: stabilizing or fading.⁴⁾ The initial pulse packet is not sharp enough in the example shown in Fig. 2(a). Therefore, the pulse packet fades away by the fifth layer. Now, how can we change the fate of the pulse packet with the inhibitory modulatory input? When the inhibitory input is sent to the second layer simultaneously with the arrival of the pulse packet, ($\Delta t = 0$ ms), the pulse packet fades away sooner, already by the second layer (Fig. 2(b)). However, when the same inhibitory input is sent slightly before the arrival of the pulse packet, $\Delta t = -6$ ms, the pulse packet is enhanced, i.e., switched to the stable mode of propagation (Fig. 2(c)). This paradoxical enhancement never occurs if the inhibitory input is sent after the arrival of the pulse packet.

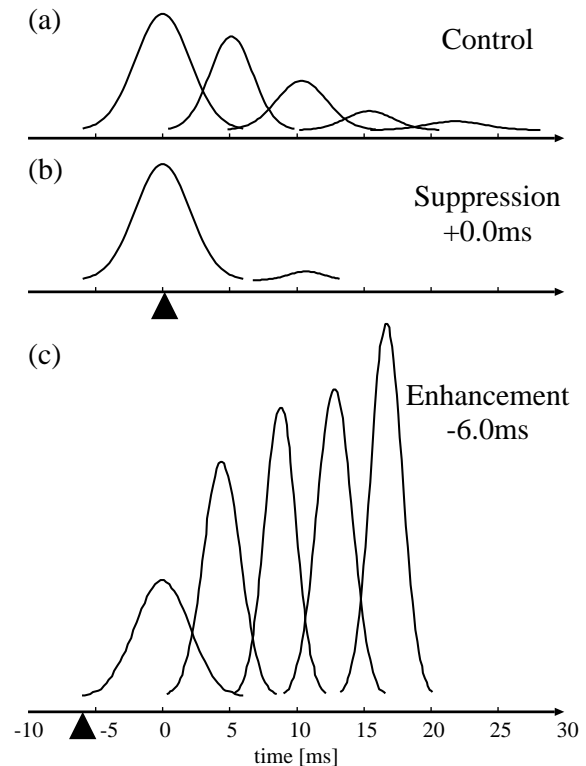


Fig. 2. Pulse packet propagation can be enhanced or suppressed by the inhibitory modulatory input. (a) A pulse packet with insufficient synchrony fades away by the fifth layer. Triangles show the timing of the inhibitory synaptic input relative to the arrival of the pulse packet. (b) The inhibitory input is given at the time of the arrival of the pulse packet ($\Delta t = 0$ ms). (c) The inhibitory input is given prior to the arrival of the pulse packet ($\Delta t = -6$ ms).

We characterized the effects of the inhibitory and excitatory modulations on the synfire chain by systematically varying the timing of the modulatory input between

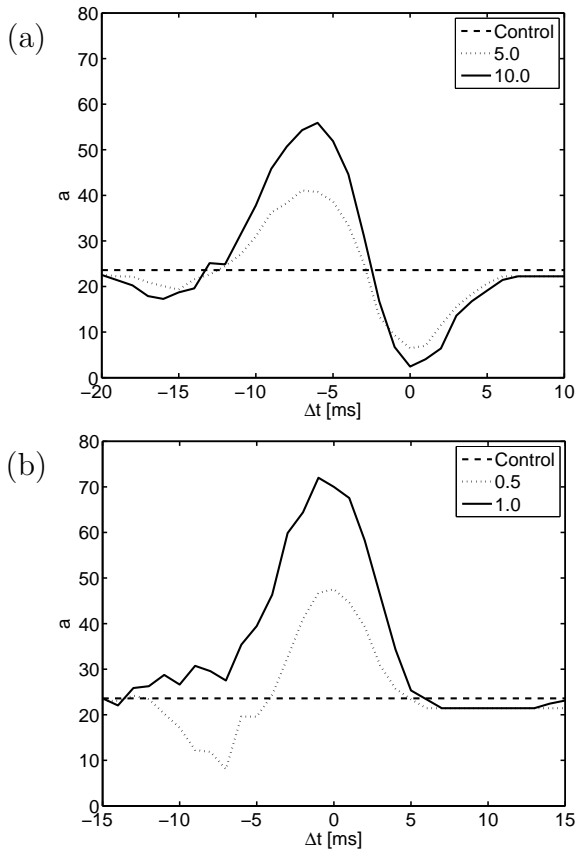


Fig. 3. Enhancement and/or suppression of a pulse packet by inhibitory(a)/excitatory(b) input depend on timing. The input pulse packet is characterized by $(\sigma, a) = (2 \text{ ms}, 40)$. By sending the inhibitory input, the pulse packet is maximally enhanced at $\Delta t = -6 \text{ ms}$ and maximally suppressed at $\Delta t = 0 \text{ ms}$.

$\Delta t = -20 \text{ ms}$ and $\Delta t = 10 \text{ ms}$. The total area of the output pulse packet gradually changed as a function of Δt (Fig. 3(a)). The population activity was maximally enhanced when the inhibitory input was sent 6 ms prior to the arrival of the pulse packet and the enhancement was seen robustly for a 10 ms range of the timing difference. We note that the enhancement strongly depended on the input amplitude but the suppression did not.

In contrast to the bidirectional control by the inhibitory input, the excitatory input worked almost unidirectionally (Fig. 3(b)). A more serious issue than the low flexibility of the excitatory modulation is that the excitatory input itself determines the timings of the output pulse packet, overriding the timing information carried by the propagating pulse packet. As we see in Fig. 4, when the excitatory input was used as a modulator, the timing of the output pulse packet was totally determined by the timing of the modulation signal, so that the timing information carried by the propagating pulse packet was lost. Thus, the excitatory modulation did not stay in the modulatory role and could not be an ideal modulator. In contrast, the timing of the output packet only weakly depended on the timing of the inhibitory modulation so that the timing of the input pulse packet was well preserved.

In order to clearly observe the influence of the in-

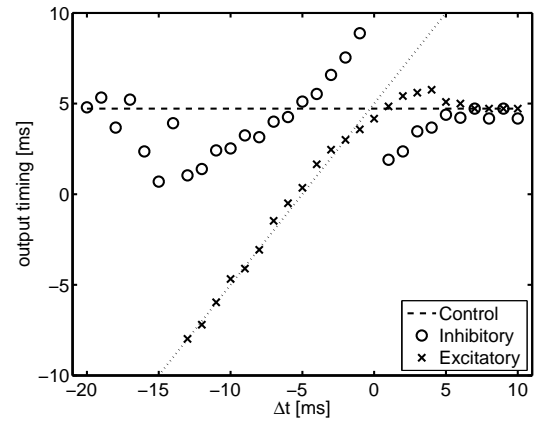


Fig. 4. The timing at which the output pulse packet is sent depends largely on the timing of the excitatory modulatory input but not on the inhibitory modulatory input. The center of the output pulse packet calculated as the mean spike times is plotted against Δt of the excitatory(crosses)/inhibitory(circles) modulatory input.

hibitory input on the dynamics of the propagation of pulse packets, we determined a flow diagram in the (σ, a) space^{4,5} showing input-output changes in the shape of the pulse packet. Figure 5 shows the successive changes $(\sigma, a) \rightarrow (\sigma', a')$ by arrows. The lengths of the arrows are normalized to a constant length for clarity. The conductance of the inhibitory input was 6.0 nS.

Under the control condition without the inhibitory modulatory input (Fig. 5(a)), the flow diagram turned out to be similar to that obtained previously with the network composed of the leaky integrate-and-fire (LIF) model.^{4,5} On the other hand, when the layer received the inhibitory input 6 ms prior to the arrival of the pulse packet, the basin of attraction was greatly enlarged, thereby enabling the synfire chain to propagate stably in much wider conditions (Fig. 5(b)). When the layer received the inhibitory input simultaneously with the arrival of the pulse packet, the synfire chain was never stabilized (Fig. 5(c)).

The enhancement of the population activity by the prior inhibitory input can be understood from a single-neuron property of the HH model.²⁶⁻²⁹ The HH neuron has an outward rectifier potassium current, which becomes active with the depolarization and terminates a spike. This outward rectifier current, which is partially active even at rest, is diminished significantly by hyperpolarization due to the prior inhibitory input, thereby making the membrane hyperactive, leading to the enhanced population activity.

Dodla and Rinzel^{28,29} have illustrated the essence of this enhancement effect from the viewpoint of a dynamical system by using the reduced HH model, in which the dynamical state is represented by the membrane voltage V and the amplitude of the potassium current n . In the V - n space, the firing threshold is represented as a curve that surrounds the lower-half of the stable attractor representing the resting state. The membrane state sitting at the attractor is kicked toward this “threshold” curve by the inhibitory input. After the kick, the mem-

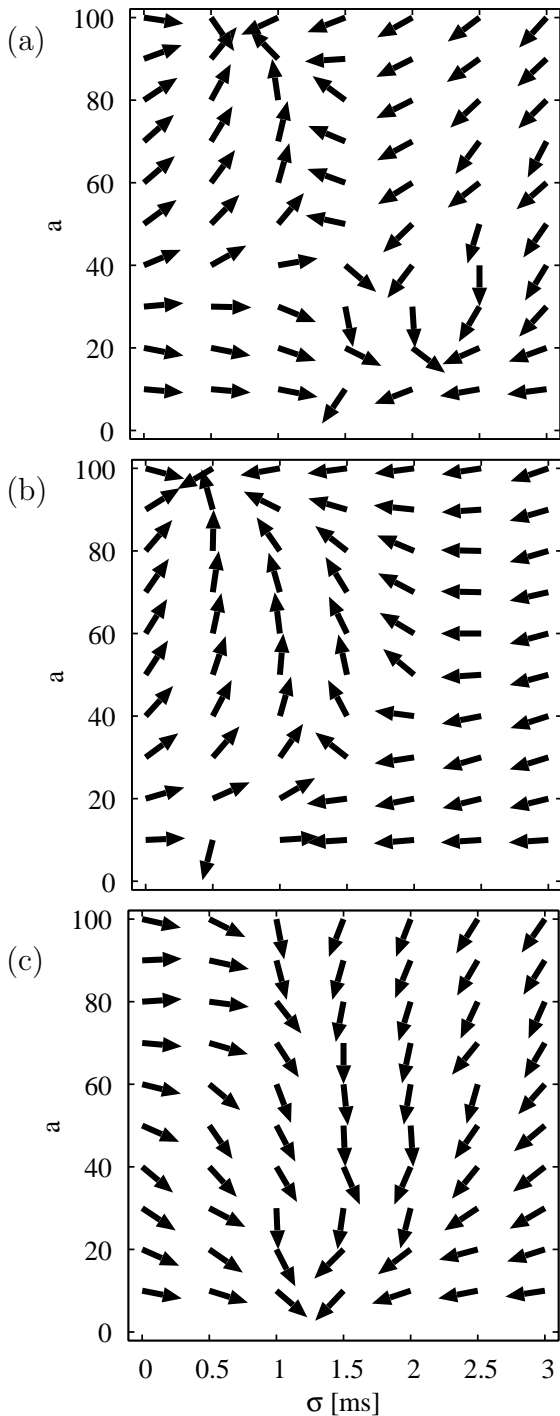


Fig. 5. Flow diagram showing the successive changes in the parameters σ and a of a pulse packet from one layer to the next. Each arrow represents the vector $(\sigma' - \sigma, a' - a)$ with its length normalized to a constant value. (a) Control condition without inhibitory modulatory input. (b) The inhibitory input was given 6 ms prior to the arrival of the pulse packet. (c) The inhibitory input was given simultaneously with the arrival of the pulse packet.

brane state moves around by maintaining contact with the threshold curve, so that the following excitatory input can easily kick the membrane state point out of the threshold curve, resulting in a spike.

We confirmed this mechanism not by reducing the HH model but by projecting the full-four dimensional HH dynamics onto the V - n plane. Figure 6 illustrates such

projections of the dynamical trajectory of the HH neuron from -10 ms to $+10$ ms, which receives a weak pulse packet $(\sigma, a) = (2 \text{ ms}, 40)$ (b) with and (a) without the prior inhibitory input at $t = -6$ ms. Only when the inhibitory input was given did the trajectory cross the “threshold manifold” which should exist as a curved plane surrounding the space below the attractor, resulting in a large overshooting trajectory representing a spike (Fig. 6(b)). Without the prior inhibitory input, the trajectory was confined in the basin of attraction (Fig. 6(a)).

Unlike previous studies, our study has determined the state points of a hundred neurons moving across the state space. We overlay all the hundred trajectories in the V - n plane and quantify how many times each point is passed by, obtaining the two-dimensional plot for the existence probability shown in Fig. 7. In other words, these figures are the histograms of the trajectories. Figure 7 clearly shows the population level influence of the inhibitory modulatory input. Without the inhibitory modulation, the state points travel around the point attractor at $(V, n) = (-63 \text{ mV}, 0.34)$, forming a crowd (Fig. 7(a)). When the inhibitory modulatory input is given, the neural population is pushed in the lower left direction approaching the threshold manifold. Many neurons can, therefore, fire when the pulse packet from the previous layer arrives at around $t = 0$ ms (Fig. 7(b)). Although the action potential trajectories are largely spread (Fig. 6), their contributions are diluted and invisible in the contour plot (Fig. 7(a)(b)). However, their movements to the lower left direction are compact and clearly reflected in the shift of the existence probability. Figure 7(c) shows the difference between Figs. 7(a) and 7(b) and clearly exposes the temporal shift by the inhibitory input.

4. Summary and discussion

The high stability of the synfire chain has been frequently examined in theoretical studies. However, to enable the synfire chain to play a major role in processing information in the brain, flexible control of its traffic is important. With such traffic control, pulse packets can reach many different parts of the brain and interact with the right partners. The present study demonstrated that an inhibitory input rather than an excitatory one most appropriate as a modulator of a pulse packet because it can bidirectionally control the pulse packet without disturbing the timing information carried by the pulse packet. In contrast, excitatory input turned out to be a poor modulator because it controlled the traffic primarily in a unidirectional manner and overrode and erased the timing information carried by the propagating pulse packet.

More importantly, only when a neuron is modeled with sufficient biological reality can the inhibitory input control the synfire chain bidirectionally. Therefore, the bidirectional control has not been investigated in studies of the synfire chain, which are based on the LIF model.^{4,5)} Unlike the LIF and FitzHugh-Nagumo models, biologically inspired models such as the HH model generally have an outward rectifying current that increases with depolarization and terminates a spike. The inhibitory input removes this current flowing even at rest and makes

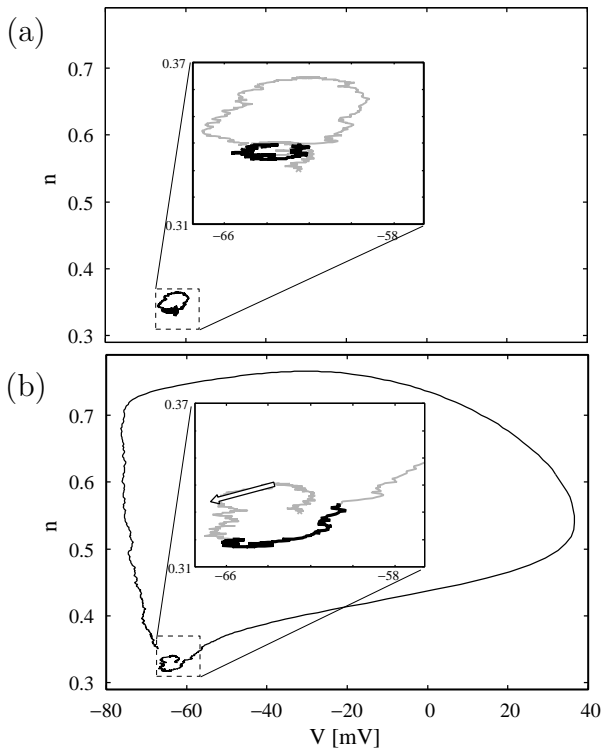


Fig. 6. Trajectories of (V, n) obtained by the simulations using the HH model. The insets show close-up views of the region around the attractor. The trajectories were drawn for $[-10 \text{ ms}, +10 \text{ ms}]$ in gray. The temporal window for the arrival of the pulse packet is indicated by a thick black line. (a) Control condition with no inhibitory input. (b) The inhibitory input was given 6 ms prior to the arrival of the pulse packet. The white arrow shows the effect of the inhibitory input.

the membrane hyperexcitable, resulting in the enhancement effect. If the same inhibitory input is given at later times, it simply suppresses the spike. This mechanism known in single-neuron studies^{26–29)} has here found renewed functional significance at a population level because the activity of the pulse packet can be controlled in a fine graded manner (Fig.3), unlike the activity of a single neuron controlled only in a binary manner: to fire or not to fire.

In the cortex where the synfire chain is supposed to be traveling, probably neurons should be described by an HH-type model rather than by the original HH model. However, the present study based on the original HH model should be relevant to the cortical neurons because the bidirectional control by the inhibitory input is a fairly universal feature in biologically inspired models, as explained above.

We have schematically illustrated the circuit in Fig. 1 for the neurons in a layer that are geometrically close to each other. However, this need not be the case and the neurons in the layer can be scattered in the brain. For our theoretical arguments, we require only the functional connectivity represented by Fig. 1. If the neurons are scattered, it is unnatural to assume that one modulatory signal serves as an input to all the neurons in a layer simultaneously. A modulatory signal should be assumed to be dispersed in time. Therefore, we perform additional

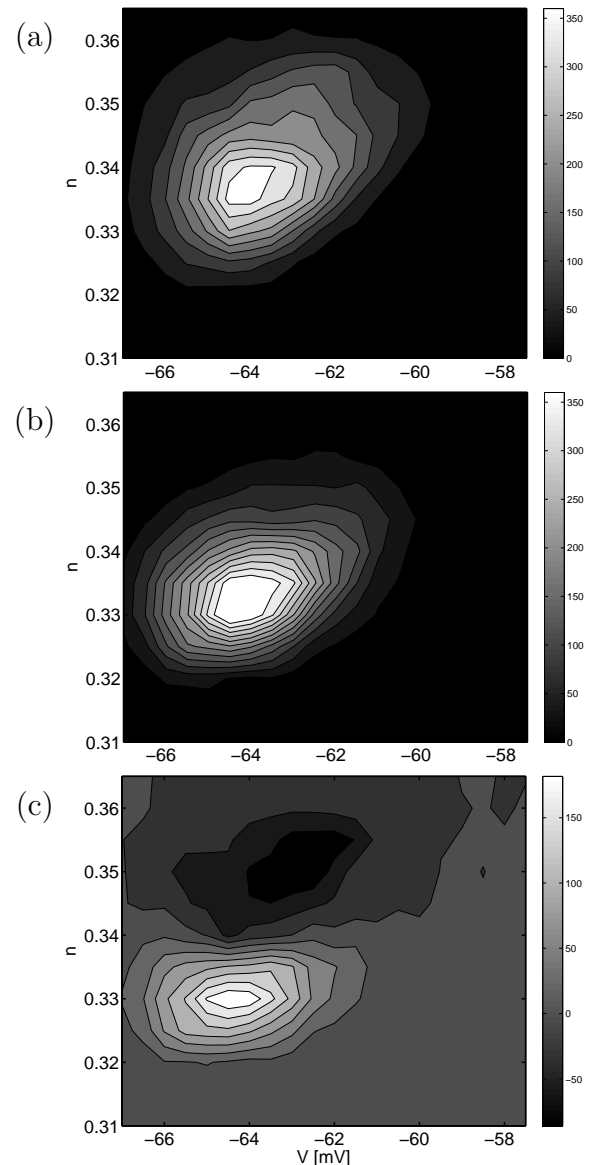


Fig. 7. Histogram of the membrane states (V, n) of the population of neurons accumulated in the time range $[-10 \text{ ms}, +10 \text{ ms}]$. (a) Neurons receive the pulse packet around $t = 0$ from the previous layer in addition to the background inputs. (b) Neurons also receive the inhibitory modulatory input at -6 ms . (c) Histogram obtained by subtracting the histogram in (a) from that in (b).

simulations by using an input that have temporal dispersion and confirm that the bidirectional control effect is minimally affected by the dispersion (Fig. 8).

Using LIF models, studies have been conducted on the control of the synfire chain. In the studies of Câteau and Fukai³⁰⁾ and Ishibashi *et al.*,¹⁴⁾ two pulse packets are simulated to interact with each other in a way possible only at the population level. Immediately after the passage of a stably propagating pulse packet, a population-refractoriness effect occurs in a layer: any pulse packet arriving at the layer is strongly suppressed. This effect does not stem from a single neuron property because it occurs even if no absolute or relative refractoriness is modeled. The population refractoriness occurs because the passage of a strong pulse packet pushes the mem-

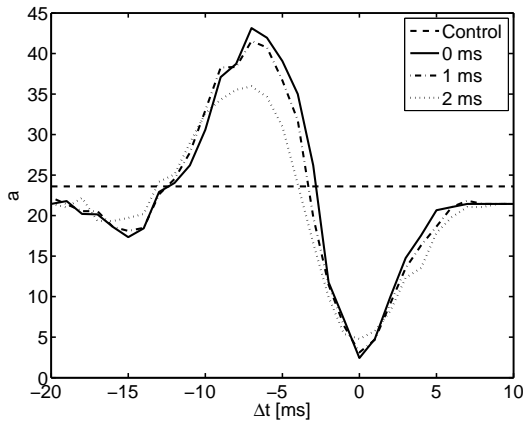


Fig. 8. Effect of the temporal variance of the inhibitory modulatory input on the enhancement and suppression of a pulse packet. The enhancement was weakened as the variance increased. However, the suppression was almost invariant under the changes in the variance.

brane potential distribution toward a lower voltage and makes the layer inactive for a while, leading to the suppression of an incoming pulse packet. The suppression effect demonstrated here is essentially distinct from the one mentioned above.

In an apparently unstructured recurrent network, the signal flow should generally be nondirectional and highly inhomogeneous: a signal flows rapidly in some parts of the network and very slowly in other parts. If the flexible control by the inhibitory input is used to suppress nondirectional flows and enhance the directional flow, it can, in principle, result in an effective feedforward circuit^{16,31} in the interconnected network. The demonstration of such an example is one of the most important topics of our future study.

Acknowledgment

This work was supported by the Special Postdoctoral Researchers Program of RIKEN.

Appendix: Neural model

The Hodgkin-Huxley neuron²⁵) was modeled as follows:

$$C_m \frac{dV}{dt} = -I_{Na} - I_K - I_L + I_{ext}, \quad (\text{A.1})$$

where $I_{Na} = \bar{g}_{Na} m_{inf}^3 h (V_{Na} - V)$, $I_K = \bar{g}_K n^4 (V_K - V)$ and $I_L = g_L (V_L - V)$ represent the sodium current, potassium current and leak current, respectively. I_{ext} $\mu\text{A}/\text{cm}^2$ is the external current input.

Gating variables ($x = h, n, m$) follow first order dynamics: $\frac{dx}{dt} = (x_{inf} - x)/\tau_x$. Here, x_{inf} and τ_x are defined as $x_{inf} = \alpha_x/(\alpha_x + \beta_x)$ and $\tau_x = \phi/(\alpha_x + \beta_x)$,

where $\phi = 0.1$ and $x = h, n, m$: $\alpha_m = -0.1(V + 40)/(\exp(-0.1(V + 40)) - 1)$, $\beta_m = 4 \exp(-(V + 65)/18)$, $\alpha_h = 0.07 \exp(-(V + 65)/20)$, $\beta_h = 1/(\exp(-0.1(V + 35)) + 1)$, $\alpha_n = -0.01(V + 55)/(\exp(-0.1(V + 55)) - 1)$, and $\beta_n = 0.125 \exp(-(V + 65)/80)$.

The membrane capacitance was set to $C_m = 1$ $\mu\text{F}/\text{cm}^2$. The values of the maximum conductance and reversal potential were set as follows: $\bar{g}_{Na} = 120$ mS/cm^2 , $\bar{g}_K = 36$ mS/cm^2 , and $g_L = 0.003$ mS/cm^2 and $V_{Na} = -55$ mV , $V_K = -80$ mV , and $V_L = -54.3$ mV .

- 1) M. Abeles: *Corticonics* (Cambridge University Press, Cambridge, 1991)
- 2) A. N. Burkitt and G. M. Clark: *Neural Comput.* **11** (1999) 871.
- 3) M. Herrmann, J. A. Hertz, and A. Prügel-Bennett: *Network* **6** (1995) 403.
- 4) M. Diesmann, M. O. Gewaltig, and A. Aertsen: *Nature* **402** (1999) 529.
- 5) H. Câteau and T. Fukai: *Neural Netw.* **14** (2001) 675.
- 6) M. C. W. van Rossum, G. G. Turrigiano, and S. B. Nelson: *J. Neurosci.* **22** (2002) 1956.
- 7) N. Masuda and K. Aihara: *Phys. Rev. Lett.* **88** (2002) 248101.
- 8) Y. Sakai: *Biosystems* **67** (2002) 221.
- 9) K. Kitano, H. Cateau, and T. Fukai: *Neuroreport* **13** (2002) 795.
- 10) A. D. Reyes: *Nat. Neurosci.* **6** (2003) 593.
- 11) K. Kitano, H. Okamoto, and T. Fukai: *Biol. Cybern.* **88** (2003) 387.
- 12) H. Câteau and A. D. Reyes: *Phys. Rev. Lett.* **96** (2006) 058101.
- 13) K. Hamaguchi, M. Okada, M. Yamana, and K. Aihara: *Neural Comput.* **17** (2005) 2034.
- 14) K. Ishibashi, K. Hamaguchi, and M. Okada: *J. Phys. Soc. Jpn.* **75** (2006) 114803.
- 15) M. Abeles, H. Bergman, E. Margalit, and E. Vaadia: *J. Neurophysiol.* **70** (1993) 1629.
- 16) J. M. Beggs and D. Plenz: *J. Neurosci.* **23** (2003) 11167.
- 17) Y. Ikegaya, G. Aaron, R. Cossart, D. Aronov, I. Lampl, D. Ferster, and R. Yuste: *Science* **304** (2004) 559.
- 18) A. Aertsen, M. Diesmann, and M. O. Gewaltig: *J. Physiol. Paris.* **90** (1996) 243.
- 19) M. Yamana and M. Okada: *J. Phys. Soc. Jpn.* **74** (2005) 2260.
- 20) K. Ishibashi, K. Hamaguchi, and M. Okada: *IEICE Tech. Rep., NC2005-171* (2005) [in Japanese].
- 21) C. Mehring, U. Hehl, M. Kubo, M. Diesmann, and A. Aertsen: *Biol. Cybern.* **88** (2003) 395.
- 22) J. Teramae and T. Fukai: to be published in *J. Comput. Neurosci.*
- 23) J. Teramae and T. Fukai: *Phys. Rev. E* **75** (2007) 011910.
- 24) M. Hines: *Int J. Biomed. Comput.* **24** (1989) 55.
- 25) A. L. Hodgkin and A. F. Huxley: *J. Physiol.* **117** (1952) 500.
- 26) W. K. Luk and K. Aihara: *Biol. Cybern.* **82** (2000) 455.
- 27) J. Feng and G. Wei: *J. Phys. A* **34** (2001) 7493.
- 28) R. Dodla and J. Rinzel: *Phys. Rev. E* **73** (2006) 010903.
- 29) R. Dodla, G. Svirskis, and J. Rinzel: *J. Neurophysiol.* **95** (2006) 2664.
- 30) H. Câteau and T. Fukai: *Neural Comput.* **15** (2003) 597.
- 31) J. M. Beggs and D. Plenz: *J. Neurosci.* **24** (2004) 5216.